International Journal of Quantum Information
Vol. 15, No. 8 (2017) 1740016 (11 pages)

DOI: 10.1142/S0219749917400160

Homodyne-like detection scheme based on photon-number-resolving detectors

Alessia Allevi

Department of Science and High Technology, University of Insubria, via Valleggio 11, Como 22100, Italy
alessia.allevi@uninsubria.it

Matteo Bina

Quantum Technology Lab, Department of Physics, University of Milan, via Celoria 16, Milano 20133, Italy
matteo.bina@unimi.it

Stefano Olivares

Quantum Technology Lab, Department of Physics, University of Milan and INFN, Sezione di Milano, via Celoria 16, Milano 20133, Italy
stefano.olivares@fisica.unimi.it

Maria Bondani*

Institute for Photonics and Nanotechnologies, National Research Center, via Valleggio 11, Como 22100, Italy
maria.bondani@uninsubria.it

Received 28 September 2017
Accepted 10 November 2017
Published 12 December 2017

Homodyne detection is the most effective detection scheme employed in quantum optics to characterize quantum states. It is based on mixing at a beam splitter the signal to be measured with a coherent state, called the "local oscillator," and on evaluating the difference of the photocurrents of two photodiodes measuring the outputs of the beam splitter. If the local oscillator is much more intense than the field to be measured, the homodyne signal is proportional to the signal-field quadratures. If the local oscillator is less intense, the photodiodes can be replaced with photon-number-resolving detectors, which have a smaller dynamics but can measure the light statistics. The resulting new homodyne-like detector acquires a hybrid nature, being it capable of yielding information on both the particle-like (statistics) and wave-like (phase) properties of light signals. The scheme has been tested in the measurement of the

*Corresponding author.

quadratures of coherent states, bracket states and phase-averaged coherent states at different intensities of the local oscillator.

Keywords: Quantum optics; light detectors; light statistics.

1. Introduction

The approach to the measurement of quantum states of light essentially follows two different strategies, which address two complementary aspects of light: homodyne detection (HD)[1] and direct detection (DD).[2] With HD, the wave-like properties of the states are exploited and a full reconstruction of the state is achieved by applying tomographic reconstruction algorithms.[3] On the other side, with DD the particle-like characteristics of light are explored and the light is described through its photon-number statistics.[4–14]

HD schemes are based on the interference of the signal to be measured with an intense coherent state, called the local oscillator (LO). The interference is obtained by mixing the two fields at a balanced beam splitter (BS). The two fields exiting the BS are detected by two pin photodiodes. The homodyne signal is given by the difference of the two pin photocurrents recorded as a function of the LO phase. To reconstruct the photon-number statistics, DD schemes employ either on/off detectors, namely detectors that can only discriminate between the presence and the absence of light (such as avalanche photodetectors, photomultipliers and single-photon nanowires), which measure single photons and are commonly used in the case of continuous-wave fields, or photon-number-resolving (PNR) detectors, which can discriminate the number of photons and are used for pulsed fields.

The homodyne-like detection scheme we analyze in this paper is based on the idea of substituting the pin photodiodes with PNR detectors in a homodyne detection scheme.[15–22] Since the operation range of PNR detectors is limited to 50–60 detected photons, their application in HD is limited to the cases of rather weak LO, so that the new scheme cannot be completely equivalent to the standard one.

We start our paper by reviewing the basic theory underlying our experiment. Then, we show the experimental results concerning coherent states and mixtures of coherent states, which exhibit exotic features. Finally, we close our analysis and draw some concluding remarks.

2. Theory

The standard homodyne scheme essentially consists of an interferometric scheme including a single balanced BS. The field to be measured, let's call it the signal mode $\hat{a}$, interferes at the BS with a reference field, the LO mode $\hat{b}$. The signal can be in any quantum state, while the LO is usually in a coherent state. If we call $\hat{c}$ and $\hat{d}$ the two BS outputs, they are linked to the input fields by

$$\hat{c} = \frac{1}{\sqrt{2}}(\hat{a} - \hat{b}); \quad \hat{d} = \frac{1}{\sqrt{2}}(\hat{a} + \hat{b}). \tag{1}$$

The key point of homodyne schemes is the evaluation of the difference between the photocurrents, namely

$$\hat{I}_c - \hat{I}_d = \hat{c}^\dagger \hat{c} - \hat{d}^\dagger \hat{d} = \hat{a}^\dagger \hat{b} + \hat{a}\hat{b}^\dagger. \tag{2}$$

If the LO is a fixed coherent state $|\beta e^{i\phi}\rangle$, we can define the *rescaled* difference photocurrent

$$\Delta\hat{I} = \frac{\langle \beta e^{i\phi}|(\hat{I}_c - \hat{I}_d)|\beta e^{i\phi}\rangle}{\sqrt{2}\beta} = \frac{\hat{a}^\dagger e^{i\phi} + \hat{a}e^{-i\phi}}{\sqrt{2}} \equiv \hat{x}_\phi, \tag{3}$$

where $\hat{x}_\phi$ is the so-called quadrature operator, ϕ being the quadrature phase. It is worth noting that the second moment of the difference photocurrent reads

$$\Delta\hat{I}^2 = \frac{\langle \beta e^{i\phi}|(\hat{I}_1 - \hat{I}_2)^2|\beta e^{i\phi}\rangle}{2\beta^2} \equiv \hat{x}_\phi^{\,2} + \frac{\hat{a}^\dagger \hat{a}}{2\beta^2} \tag{4}$$

and that similar results can be obtained for higher-order moments of $\Delta\hat{I}$.[23] The standard result of HD, that is the measurement of $\hat{x}_\phi$, is therefore obtained in the limit $\beta^2 \gg \langle \hat{a}^\dagger \hat{a}\rangle$, i.e. when the LO is much more intense (macroscopic) than the input signal. However, in the presence of low-intensity LO, the difference photocurrent (3) does not correspond anymore to the measurement of the quadrature operator. We will refer to this case as the homodyne-like configuration.
In the following we are going to consider the homodyne and the homodyne-like configurations for different signal states.

2.1. *Coherent states*

When the signal mode $\hat{a}$ is in the coherent state $|\alpha\rangle$, $\alpha \in \mathbb{R}$, and the LO is macroscopic, the homodyne distribution of the quadrature $\hat{x}_\phi$ reads as[23]

$$p_{\mathrm{HD}}(x;\alpha;\phi) = p_\phi(x;\alpha) = \frac{1}{\sqrt{\pi}} \exp\Big[-(x - \sqrt{2}\alpha\cos\phi)^2\Big], \tag{5}$$

i.e. it is a normal distribution with mean $\langle x\rangle = \sqrt{2}\alpha\cos\phi$ and variance $\sigma_x^2 = 1/2$. To evaluate the analog of Eq. (5) in the case of a LO with generic intensity, we consider a signal mode in the coherent state $|\alpha\rangle$ mixed with a LO $|\beta e^{i\phi}\rangle$. Each output of the BS is described by a Poisson distribution of the number of photons, whose mean value is either $\mu_1 = \frac{1}{2}(\alpha^2 + \beta^2) + \alpha\beta\cos\phi$ or $\mu_2 = \frac{1}{2}(\alpha^2 + \beta^2) - \alpha\beta\cos\phi$ depending on which output is considered.

The distribution of the difference d of photon numbers can be evaluated as the convolution of the two Poisson distributions and is described by the Skellam distribution[24]

$$S(d;\alpha;\phi) = e^{-\mu_1-\mu_2}\left(\frac{\mu_1}{\mu_2}\right)^{d/2} I_d(2\sqrt{\mu_1\mu_2}), \tag{6}$$

in which $I_d(x)$ is the modified Bessel function of the first kind. Note that $\mu_{1,2} = \mu_{1,2}(\alpha;\beta;\phi)$. Hence, for the homodyne-like probability distribution obtained by performing DD we have

$$p_{\mathrm{DD}}(d;\alpha;\phi) = S(d;\alpha;\phi). \tag{7}$$

We note that when the LO is very intense, $\beta \gg |\alpha|$, it is easy to show that $p_{\mathrm{DD}}(d;\alpha;\phi) \to p_{\mathrm{HD}}(x = d/(\sqrt{2}\beta);\alpha;\phi)/(\sqrt{2}\beta)$.

2.2. *Bracket states*

The results obtained for a coherent state as the signal can be extended to the case of mixtures of coherent states, such as the so-called bracket states, made by the statistical mixture of two coherent states with opposite phases.[25,26] The homodyne distribution for a bracket state can be written as

$$p_{\mathrm{HD}}(x;\alpha;\phi) = \frac{p_{\phi}(x;\alpha) + p_{\phi+\pi}(x;\alpha)}{2}, \tag{8}$$

while the case of DD, which holds for a generic LO, can be written as:

$$p_{\mathrm{DD}}(d;\alpha;\phi) = \frac{S(d;\alpha;\phi) + S(d;\alpha;\phi+\pi)}{2}. \tag{9}$$

2.3. *Phase-averaged coherent states*

If we now consider a continuous mixture of coherent states with phases uniformly distributed in $[0, 2\pi]$, that is the so-called phase-averaged coherent state,[21] the homodyne distribution becomes

$$p_{\mathrm{HD}}(x;\alpha) = \frac{1}{2\pi}\int_0^{2\pi} d\phi p_{\phi}(x;\alpha), \tag{10}$$

while the DD counterpart can be written as:

$$p_{\mathrm{DD}}(d;\alpha) = \frac{1}{2\pi}\int_0^{2\pi} d\phi S(d;\alpha;\phi). \tag{11}$$

3. Experimental Setup

We tested the proposed homodyne-like detection scheme with the setup shown in Fig. 1. Both the signal field and the LO were obtained from the second-harmonic pulses (5-ps-pulse duration) emitted at 523 nm by a mode-locked Nd:YLF laser regeneratively amplified at 500 Hz. The two fields were sent to a Mach–Zehnder interferometer, in which the first BS prepares the fields and the second one realizes the interference for the homodyne scheme. Two variable neutral density filters inserted in the two arms of the interferometer were used to change the balancing

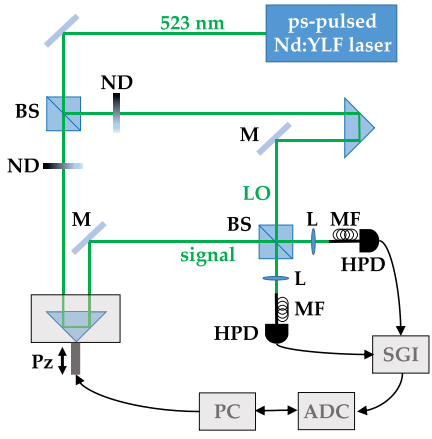

Fig. 1. Sketch of the experimental setup. BS: beam splitter; ND: variable neutral density filters; Pz: piezoelectric movement; MF: multi-mode fibers; HPD: hybrid photodetectors; M: plane mirrors; L: converging lenses; SGI: synchronous-gated integrator; ADC: analog-to-digital converter; PC: computer.

between the two fields. The spatial and temporal superpositions of signal and LO were optimized to get the optimal overlap between signal and LO.

The phase between signal and LO was modified in steps by changing the length of one of the arms of the interferometer by means of a piezoelectric movement. We set 60 different piezo positions and for each one we recorded 50000 laser shots. The data measured at each piezo position correspond to coherent states having the same amplitude but different phases. Post-processing the data corresponding to a combination of phases allows the production of bracket states and phase-averaged coherent states, as explained below.

The light at the two outputs of the second BS was collected by two multi-mode fibers (600-μm-core diameter) and sent to two hybrid photodetectors (HPDs, mod. R10467U-40, Hamamatsu). The output of each detector was amplified (preamplifier A250 plus amplifier A275, Amptek), synchronously integrated over a 500-ns window (SGI, SR250, Stanford) and digitized (AT-MIO-16E-1, National Instruments). The HPDs belong to the class of PNR detectors and have a partial photon-number-resolving capability, that is the peaks in pulse-height spectrum of the detector's outputs are not perfectly resolved. In spite of the non-perfect photon-number resolution of the detectors, we have demonstrated[8,27] that a suitable analysis of the outputs enables the reconstruction of the photon statistics of trivial and non-trivial optical states.[28,29] According to the analysis presented in Refs. 8 and 27, the detection process of HPDs can be modeled by two steps: photodetection by the photocathode and amplification. The first process is described by a Bernoullian convolution, while the second one by the multiplication by a constant factor γ. The value of this factor can be obtained either through a self-consistent method directly based on the measured light or evaluating the distance between two consecutive valleys in the pulse-height spectrum of the detector output. Once the value of γ has been determined, the

number of detected photons is obtained by dividing the output voltages (typically a few volts), previously subtracted of the mean value of the electronic noise, by the factor γ and then rebinning the results in unitary bins. The procedure establishes a correspondence between output voltages and detected photons at any single shot. Since HPDs have a linear response to the incident power up to 80 detected photons, the procedure directly gives the information about the mean values of the detected light without any need of separate calibration.

From the direct measurement of the mean values, the relative phase ϕ can be estimated.[26,30] In fact, the mean number of photons detected at each output of the interferometer follows the interference pattern as a function of the delay set by the piezo movement. The information on the phases is necessary both to evaluate the theoretical models to be superimposed to the experimental data and to build some of the states, like bracket states and phase-averaged coherent states.

The relative phase between the two arms of the interferometer can be retrieved by interpreting the mean values measured at the outputs as the result of an interference process, even if irregular. From the mean values, the experimental value of $\cos(\phi)$ is directly extracted and the phase evaluated. In Fig. 2, a typical result of a

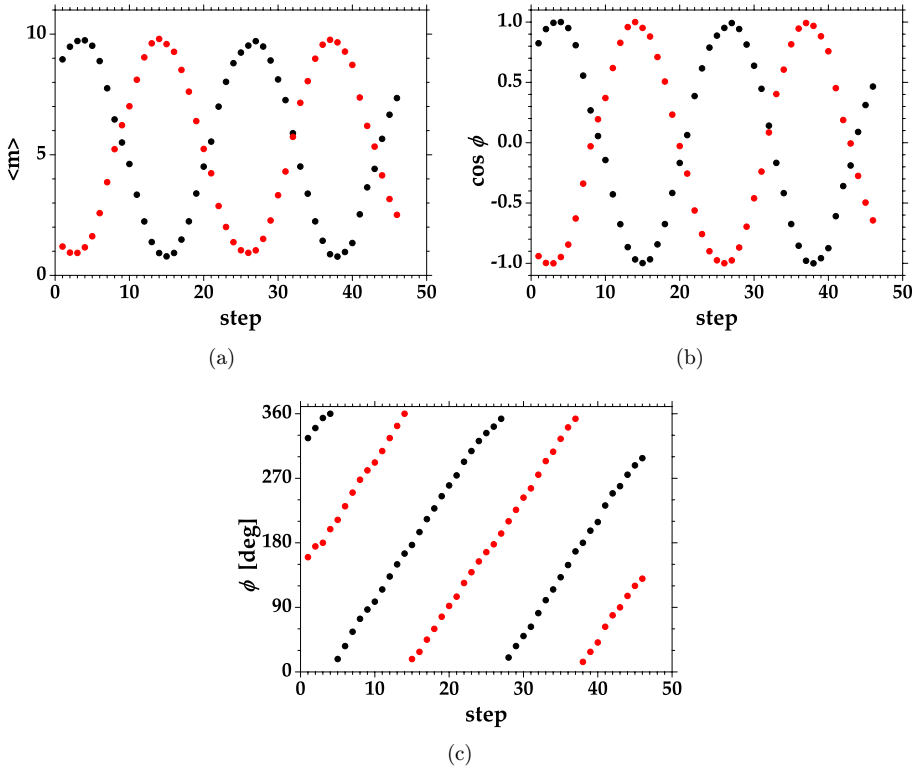

Fig. 2. (a) Mean values of detected photons at the two BS outputs, (b) Calculated values of $\cos\phi$, and (c) Estimated values of ϕ. All the quantities are plotted as functions of the piezo position.

measurement is displayed. Once the values of phases are determined, bracket states are obtained by appending the dataset corresponding to a fixed value of the phase together with the dataset corresponding to the same phase shifted by π. In a similar way, phase-averaged coherent states are produced by combining in a unique file the data corresponding to all the phase values. We note that the phase-averaged state generated in the experiment is only an approximation of the ideal phase-averaged state since the number of independent phases is limited to 60. Nevertheless, the phase-averaged state we produced has a good quality because of the uniformity of the distribution of the composing phases. Typical reconstructions of the photon-number statistics p_m registered by the detectors are shown in Fig. 3 for coherent states (panel (a)), bracket states (panel (b)), and phase-averaged coherent states (panel (c)). The experimental values are displayed as dots, while the theoretical expectations as full lines. We notice that for almost all the cases, the theoretical distributions are well superimposed to the experimental data with a very high fidelity

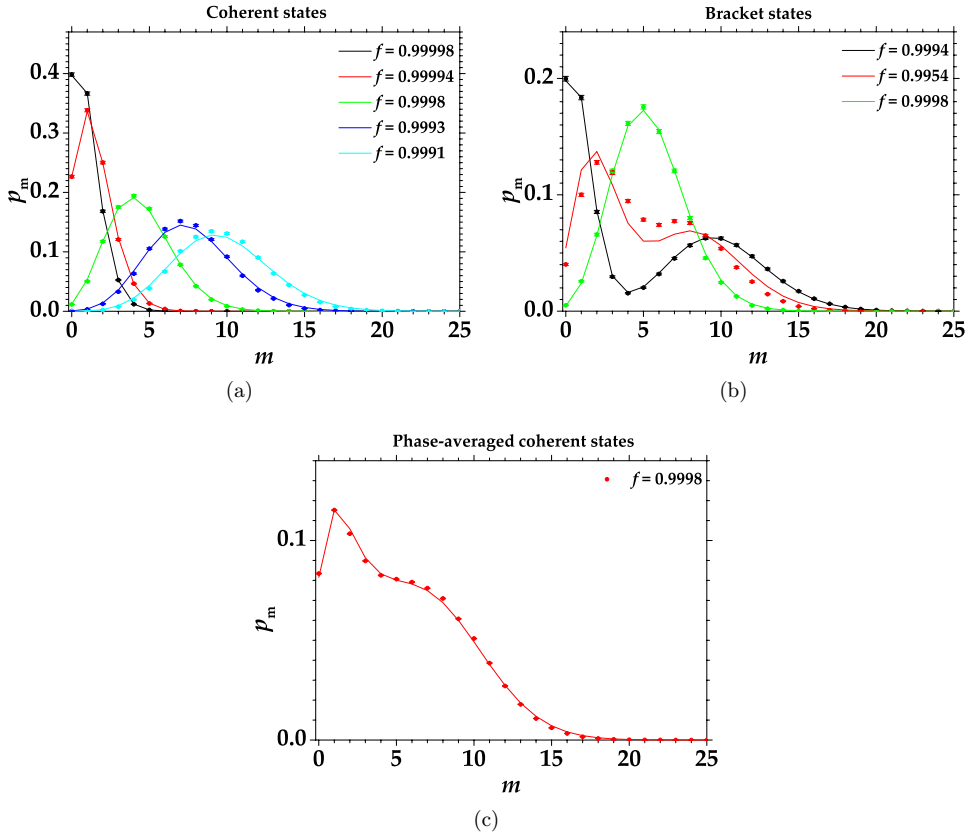

Fig. 3. Reconstruction of detected-photon distributions p_m measured at one BS output. (a) Coherent states at different values of the LO phase, (b) bracket states at different values of the LO phase, and (c) phase-averaged states. Symbols: experimental data; line: theoretical expectations.

($f = \sum_m \sqrt{p_{\mathrm{exp},m} p_{\mathrm{theor},m}}$, with $p_{\mathrm{exp},m}$ the experimental statistics and $p_{\mathrm{theor},m}$ the corresponding theoretical expectation). The values of the fidelities are written in the figures.

4. Results

From the shot-by-shot measurements of the fields at the BS outputs of the HD-like detector, it is possible to evaluate the experimental difference p_d of detected-photon numbers as a function of the phase ϕ and of the amplitude β of the LO. The experimental results can be compared with the theoretical expectations described in Sec. 2 to check the validity of the general model and of the standard homodyne intense LO approximation.

We illustrate the results for coherent states in Fig. 4, for bracket states in Fig. 5 and for phase-averaged coherent states in Fig. 6. All these figures contain the experimental data (dots + error bars), the theoretical expectations for a LO having generic intensity (full lines) and the theoretical expectations for standard HD (dashed lines). For each class of states (coherent, bracket and phase-averaged), two values of the ratio $\beta^2/|\alpha|^2$, namely $\beta^2/|\alpha|^2 \sim 8$ and $\beta^2/|\alpha|^2 \sim 1$ are shown. By comparing the two panels of each figure, we note that when the signal and LO are balanced ($\beta^2/|\alpha|^2 \sim 1$) the data differ from the standard probability distribution, whereas they are very well superimposed to the theoretical expectation for low-intensity LO. On the contrary, when $\beta^2/|\alpha|^2 \sim 8$, the two probability distributions are well superimposed to each other and in perfect agreement with the experimental data.

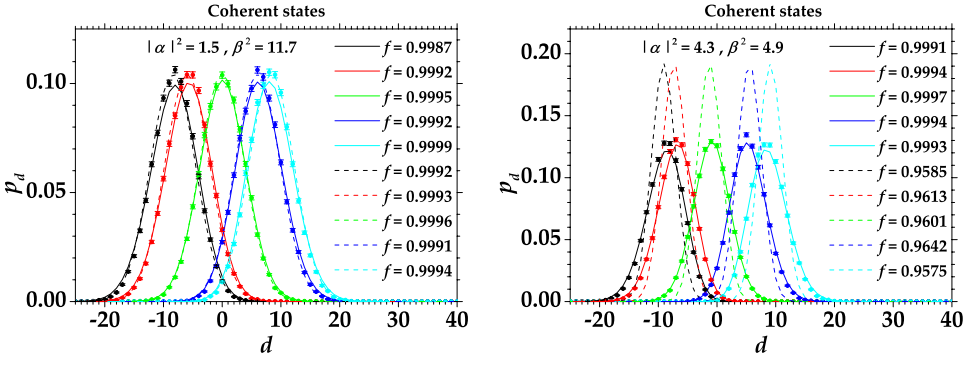

Fig. 4. Statistics p_d of the experimental difference of the outputs of the homodyne-like detection scheme in the case of a coherent-state signal for different phase values and two different balancing of signal and LO. Dots + error bars: experimental data; Full lines: theoretical expectations according to Eq. (7); Dashed lines: theoretical expectations according to Eq. (5). (a) $\phi = 3$ deg (black), $\phi = 45$ deg (red), $\phi = 90$ deg (green), $\phi = 136$ deg (blue), $\phi = 177$ deg (cyan); (b) $\phi = 0$ deg (black), $\phi = 45$ deg (red), $\phi = 90$ deg (green), $\phi = 135$ deg (blue), $\phi = 180$ deg (cyan).

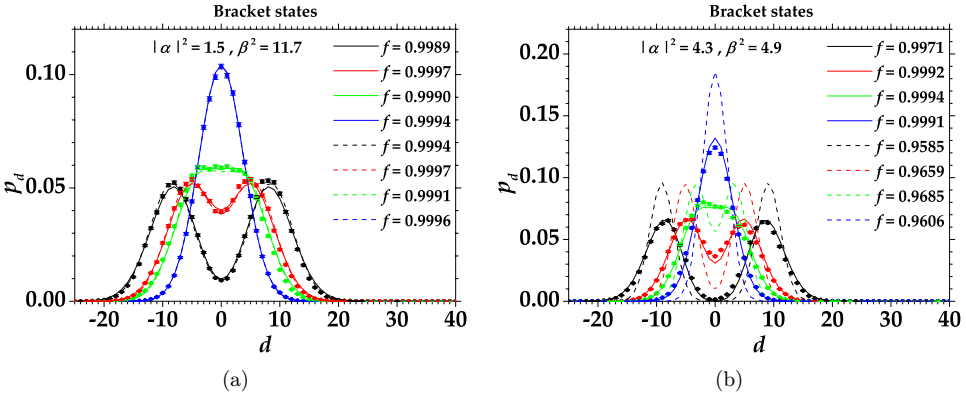

Fig. 5. Statistics p_d of the experimental difference of the outputs of the homodyne-like detection scheme in the case of a bracket-state signal for different phase values and for two different balancing of signal and LO. Dots + error bars: experimental data; Full lines: theoretical expectations according to Eq. (9); Dashed lines: theoretical expectations according to Eq. (8). (a) $\phi = 0$ deg (black), $\phi = 50$ deg (red), $\phi = 60$ deg (green), $\phi = 90$ deg (blue); (b) $\phi = 8$ deg (black), $\phi = 56$ deg (red), $\phi = 69$ deg (green), $\phi = 87$ deg (blue).

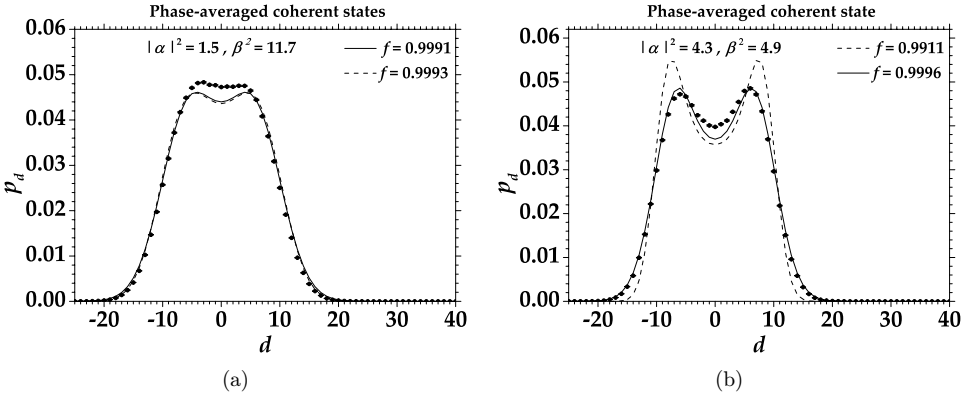

Fig. 6. Statistics p_d of the experimental difference of the outputs of the homodyne-like detection scheme in the case of the phase-averaged-coherent-state signal for two different balancing of signal and LO. Dots + error bars: experimental data; Full lines: theoretical expectations according to Eq. (11); Dashed lines: theoretical expectations according to Eq. (10).

5. Conclusion

We presented the implementation of a homodyne-like detection scheme employing PNR detectors instead of pin photodiodes. The experimental results based on coherent states and mixtures of coherent states are well interpreted by the theory. Moreover, our findings demonstrate that a homodyne-like detection scheme can be implemented using a LO with finite intensity.[31] Our scheme can give information both on the number of photons and on the wave-like properties of the states under investigation. In particular, it gives direct access to the photon-number statistics at

the two output ports and this additional information can be exploited to characterize the detected state without, e.g., performing homodyne tomography. For instance, the evaluation of the photon-number correlations at the outputs gives information about the quantum nature of the state[32] without the full processing of the homodyne data. A crucial role in this respect is played by the linearity of the detection chain, which gives access to the relative phase between signal and LO.

In conclusion, we remark that the main idea of building a novel scheme based on PNR detectors is not just to mimic the conventional HD based on pin photodiodes, but to explore what kind of increased knowledge can be achieved by using PNR detectors combined with the interferometric scheme typical of HD. In fact, we expect that the combination of DD and HD will give a more complete insight into the properties of light and will open new perspectives for the applications of light in quantum information and communication protocols.[33,34] The quality of our experimental data suggests the possible exploitation of the detection scheme for the development of protocols based on coherent states. In this light, it has been recently shown[34] that the use of this kind of detection can increase the mutual information between sender and receiver in continuous-variable quantum key distribution, thus opening the way to the development of new protocols.

References

1. A. I. Lvovsky and M. G. Raymer, *Rev. Mod. Phys.* **81** (2009) 299.
2. A. Allevi and M. Bondani, *Adv. Atom. Mol. Phys.* **66** (2017) 49.
3. G. M. D'Ariano *et al.*, *Phys. Rev. A* **58** (1998) 636.
4. E. Waks *et al.*, *Phys. Rev. A* **73** (2006) 033814.
5. M. Avenhaus *et al.*, *Phys. Rev. Lett.* **101** (2008) 053601.
6. W. Wasilewski *et al.*, *Phys. Rev. A* **78** (2008) 033831.
7. W. Mauerer *et al.*, *Phys. Rev. A* **80** (2008) 053815.
8. M. Bondani *et al.*, *J. Mod. Opt.* **56** (2009) 226.
9. M. Ramilli *et al.*, *J. Opt. Soc. Am. B* **27** (2010) 852.
10. D. A. Kalashnikov *et al.*, *Opt. Express* **19** (2011) 9352.
11. J. Peřina Jr. *et al.*, *Phys. Rev. A* **85** (2012) 023816.
12. M. Lamperti *et al.*, *J. Opt. Soc. Am. B* **31** (2014) 20.
13. A. Allevi *et al.*, *Phys. Rev. A* **88** (2013) 063807.
14. G. Harder *et al.*, *Phys. Rev. Lett.* **116** (2016) 143601.
15. S. Wallentowitz and W. Vogel, *Phys. Rev. A* **53** (1996) 4528.
16. K. Banaszek *et al.*, *Phys. Rev. A* **60** (1999) 674.
17. M. Bondani *et al.*, *Opt. Lett.* **34** (2009) 1444.
18. G. Puentes *et al.*, *Phys. Rev. Lett.* **102** (2009) 080404.
19. K. Laiho *et al.*, *Phys. Rev. Lett.* **105** (2010) 253603.
20. L. Zhang *et al.*, *Nat. Photon.* **6** (2012) 364.
21. A. Allevi *et al.*, *Opt. Express* **20** (2012) 24850.
22. G. Donati *et al.*, *Nat. Commun.* **5** (2014) 5584.
23. A. Ferraro *et al.*, *Gaussian States in Quantum Information* (Bibliopolis, Napoli, 2005).
24. J. G. Skellam, *J. Roy. Statist. Soc. (N. S.)* **109** (1946) 296.
25. A. Allevi *et al.*, *Int. J. Quant. Inf.* **12** (2014) 1461018.
26. M. Bina *et al.*, *Sci. Rep.* **6** (2016) 26025.

27. A. Andreoni and M. Bondani, *Phys. Rev. A* **80** (2009) 013819.
28. M. Bondani *et al.*, *Adv. Sci. Lett.* **2** (2009) 463.
29. A. Allevi and M. Bondani, *Opt. Lett.* **40** (2015) 3089.
30. A. Allevi *et al.*, *J. Opt. Soc. Am. B* **27** (2010) 333.
31. A. Cives-Esclop *et al.*, *Opt. Commun.* **175** (2000) 153.
32. A. Allevi *et al.*, *Phys. Rev. A* **85** (2012) 063835.
33. M. Bina *et al.*, *Opt. Express* **25** (2017) 10685.
34. M. Cattaneo *et al.*, arXiv:1707.02852.